What do global p-modes tell us about banana cells?

Piyali Chatterjee

NORDITA, AlbaNova University Center, Roslagstullsbacken 23, SE 10691 Stockholm, Sweden

E-mail: `piyalic@nordita.org`

Abstract. We have calculated the effects of giant convection cells also know as sectoral rolls or banana cells, on p-mode splitting coefficients. We use the technique of quasi-degenerate perturbation theory formulated by Lavely & Ritzwoller in order to estimate the frequency shifts. A possible way of detecting giant cells is to look for even splitting coefficients of 'nearly degenerate' modes in the observational data since these modes have the largest shifts. We find that banana cells having an azimuthal wave number of 16 and maximum vertical velocity of 180 m s^{-1} cannot be ruled out from GONG data for even splitting coefficients.

1. Introduction

The power spectra of solar convective velocities show distinct peaks representing granules and supergranules but no distinct features at wavenumbers representative of mesogranules or giant cells (Wang 1989; Chou et al. 1991; Straus and Bonaccini 1997; Hathaway et al. 2000). Numerical simulations of solar convection routinely show the existence of mesogranules and giant cells (Miesh et al. 2008, Käpylä et al. 2010). Of particular interest is the existence of sectoral rolls or 'banana cells' having maximum radial velocities of 200-300 ms^{-1}. The giant convective cells have always been elusive to observations at the solar surface. In the past there have been studies which have failed to detect giant cell motions (LaBonte, Howard and Gilman 1981; Snodgrass and Howard 1984; Chiang, Petro and Fonkal 1987) as well as those hinting at their existence (Hathaway et al. 1996; Simon and Strous 1997). With the availability of Dopplergrams from SOHO/MDI, it became possible to study such long-lived and large scale features more reliably. Beck, Duvall and Scherrer (1998) were able to detect giant cells at the solar surface with large aspect ratio (~ 4) and velocities ~ 10 m s^{-1} using the MDI data. Hathaway et al. (2000) used spherical harmonic spectra from full disk measurements to detect long-lived power at $l \leq 64$.

Are banana cells observed regularly in direct numerical simulations (DNS), real or are they an artifact of insufficient resolution? Is it possible for techniques of global helioseismology to throw any light on the existence of giant cells? Traditionally, only degenerate perturbation theory (DPT) has been used to calculate the effect of rotation on the p-modes. But the first order contribution from poloidal flows (of which giant cells are a particular case) calculated using the degenerate perturbation theory vanishes giving rise to the need to use the quasi degenerate perturbation theory (QDPT) which in contrast to DPT couples modes having slightly different unperturbed frequencies. Quasi degenerate perturbation theory was applied to calculate shifts due to flows and asphericity in solar acoustic frequencies by Lavely and Ritzwoller (1992). Roth and Stix (1999, 2003) used QDPT to calculate the effect of giant cells on p-modes and claimed that giant cells could be found by modeling the asymmetries and line broadening in the solar power spectrum. They claimed that finite line width of the multiplets would limit the detection

of the frequency splittings to vertical velocity amplitude of 100 m s^{-1} or larger. In Chatterjee and Antia (2009, CA09 now onwards), we used a different approach to examine if the use of quasi degenerate perturbation theory introduces significant corrections in the frequency shifts over that obtained from degenerate perturbation theory. We found the effect of rotation on the odd coefficients is negligible and hence using the degenerate theory is sufficient. Additionally, CA09 also calculated the effect of N-S asymmetric component of rotation, single cell meridional circulation, giant cells and banana cells on p-modes. We also showed that for higher angular degree of the poloidal flows, the 'nearly degenerate' modes would have very large frequency shifts (splitting coefficients). It is these splitting coefficients we can hope to detect in observational data.

In this paper we present results for banana cells but with an angular degree twice that used in CA09. In Sect. 2, we present a brief description of the method for completeness. In Sect. 3 we present the results of our calculations and draw conclusions in Sect. 4.

2. Perturbation of p- & f-modes by giant cells

Any perturbation calculation first requires definition of a base state with unperturbed eigenfrequencies as well as eigenvectors denoted ω_k and $\mathbf{s_k}$ respectively, which we shall call non-rotating spherically symmetric (NRSS) state. In this work we have used a standard solar model with the OPAL equation of state (Rogers and Nayfonov 2002) and OPAL opacities (Iglesias and Rogers 1996) and use the formulation due to Canuto and Mazitelli (1991) to calculate the convective flux. The equations of motion for a mode k with eigenfrequency ω_k for a NRSS model and a model perturbed by addition of differential rotation and/or large scale flow can be respectively represented by,

$$\mathcal{L}_0 \mathbf{s_k} = -\rho_0 \omega_k^2 \mathbf{s_k}, \tag{1}$$

$$\mathcal{L}_0 \mathbf{s'_k} + \mathcal{L}_1 \mathbf{s'_k} = -\rho_0 {\omega'_k}^2 \mathbf{s'_k}, \tag{2}$$

where ω'_k is the perturbed frequency and $\mathbf{s'_k} = \sum_{k' \in K} a_{k'} \mathbf{s_{k'}}$ is the perturbed eigenvector. Taking scalar product with $\mathbf{s_j}$ in equation (2) and using the notation $\mathcal{H}_{jk'} = -\int \mathbf{s_j}^\dagger \mathcal{L}_1 \mathbf{s_{k'}} dV$ and the definition $\mathcal{L}_1 \mathbf{s_k} = -2i\omega_{\mathrm{ref}} \rho_0 (\mathbf{v}.\nabla) \mathbf{s_k}$, we obtain the matrix eigenvalue equation,

$$\sum_{k' \in K} \left\{ \mathcal{H}_{jk'} + \delta_{k'j} (\omega_{k'}^2 - \omega_{\mathrm{ref}}^2) \right\} a_{k'} = ({\omega'_k}^2 - \omega_{\mathrm{ref}}^2) a_j, \tag{3}$$

with eigenvalue $\lambda = ({\omega'_k}^2 - \omega_{\mathrm{ref}}^2)$ and eigenvector $X_j = \{a_j\}$. Here ω_{ref} is a reference frequency which approximates ω'_k. In this work we use $\omega_{\mathrm{ref}} = \omega_k$, the frequency of the mode being perturbed. For details on calculation of the matrix elements, the reader is referred to Sect. 3.2 of CA 09. Essentially we use the Wigner-Eckart theorem (equation 5.4.1 of Edmonds 1960) which states that the general matrix element of any tensor perturbation operator can be expanded in terms of Wigner $3j$ symbols whose coefficients of expansion are independent of azimuthal order m and m'.

An important thing to remember is that for two modes with frequencies ω_1 and ω_2, the frequency shift is given by,

$$\delta\nu = \frac{\omega'_2 - \omega_2}{2\pi} \sim \frac{\mathcal{H}_{12}^2}{4\pi\omega_2\Delta} \tag{4}$$

where $\mathcal{H}_{12}$ is the coupling matrix between the two modes and $\Delta = (\omega_2{}^2 - \omega_1^2)$. Traditionally in helioseismology, the frequency shift as a function of m is described in terms of splitting coefficients for all modes that are detected. These coefficients are defined by (e.g., Ritzwoller and Lavely 1991)

$$\omega_{nlm} = \omega_{nl} + \sum_{q=0} a_q^{(nl)} \mathcal{P}_q^l(m), \tag{5}$$

where ω_{nl} is the mean frequency of the multiplet, $\mathcal{P}_q^l(m)$ are the orthogonal polynomials of degree q and $a_q^{(nl)}$'s are the so called splitting coefficients. A multiplet with frequency ω_{nl} is $2l + 1$-fold degenerate in absence of rotation, magnetic field, poloidal flows and asphericity. Following earlier works (Lavely and Ritzwoller 1992; Roth, Howe and Komm 2002) we express the velocity field in terms of spherical harmonics. For completeness, we give the expression here again.

$$
\begin{aligned}
\mathbf{v}(r,\theta,\phi) &= \mathrm{Re}[u_s^t(r)Y_s^t(\theta,\phi)\hat{\mathbf{r}} + v_s^t(r)\nabla_h Y_s^t(\theta,\phi) - \\
&\quad w_s^t(r)\hat{\mathbf{r}} \times \nabla_h Y_s^t(\theta,\phi)].
\end{aligned}
\tag{6}
$$

The quantities u_s^t, v_s^t and w_s^t determine the radial profiles of the flows and ∇_h is the horizontal gradient operator. The Re refers to using only the real part of the spherical harmonics as in,

$$
\mathrm{Re}[Y_s^t(\theta,\phi)] = \begin{cases} [Y_s^{-t}(\theta,\phi) + Y_s^t(\theta,\phi)]/2 & \text{if } t \text{ is even,} \\ [Y_s^{-t}(\theta,\phi) - Y_s^t(\theta,\phi)]/2 & \text{if } t \text{ is odd.} \end{cases}
\tag{7}
$$

The first two terms in equation (6) define the poloidal component of the flow whereas the last term is the toroidal component. By the poloidal component, we imply the meridional and non-zonal toroidal flows (average over ϕ direction is zero) e.g., (i) the meridional circulation which carries mass poleward near the surface and sinks near the poles and (ii) the giant convection cells, respectively. These flows are also called large scale flows to distinguish them from other small scale flows like the turbulent eddies which are of the size smaller than the typical scale of global modes used in helioseismology.

The sectoral rolls or banana cells are characterised by $s = t$. CA09 used $s = t = 8$ for banana cells. Visual inspection of the snapshots of vertical velocity in Fig. 1 of Miesch et al. (2006) as well as Fig. 2c of Käpylä et al. (2010) reveals that banana cells observed in DNS of stellar convection has $s \sim 16, t \sim 16$. In addition Miesch et al. (2008) also put the value of the maximum radial velocity at 200 m s^{-1}. So it makes sense to repeat our calculations for a flow with an angular dependence $Y_{16}^{16}(\theta,\phi)$. In this calculation we have used only the estimate of the magnitude of maximum radial velocities and their angular degree from the DNS. The solar structure we use for frequency shift calculations come from a spherically symmetric non-rotating standard solar model (NRSS model) and the rotation splittings needed are obtained from temporally averaged GONG data. These two quantities are very different for DNS since they have much shallower density stratification and sometimes give a rotation profile which is constant on cylinders rather than cones as for the Sun. A more realistic calculation would be to use the stratification and the rotation rate from the DNS to define the unperturbed state. Nevertheless, a first calculation using a NRSS model and GONG rotation profile can provide valuable insights into the possibility of such poloidal flows.

In presence of only the poloidal flow ($w_s^t = 0$) we can apply the equation of mass conservation $\nabla.(\rho_0\mathbf{v}) = 0$ to get a relation between $u_s^t(r)$ and $v_s^t(r)$ e.g.,

$$
v_s^t(r) = \frac{1}{r}\frac{\partial}{\partial r}\left[\frac{\rho_0 r^2 u_s^t(r)}{s(s+1)}\right].
\tag{8}
$$

Here $\rho_0(r)$ is the density in a spherically symmetric solar model. So now it only remains to choose $u_s^t(r)$ appropriately and $v_s^t(r)$ will be determined by equation (8). We choose the radial profile of $u_s^t(r)$ as given by equation (19) of Roth, Howe & Komm (2002):

$$
u_s^t(r) = \begin{cases} u_0\dfrac{4(R_{\mathrm{top}} - r)(r - r_b)}{(R_{\mathrm{top}} - r_b)^2} & \text{if } r_b \leq r \leq R_{\mathrm{top}}, \\ 0 & \text{otherwise.} \end{cases}
\tag{9}
$$

Here $r_b = 0.7R_\odot$ and $R_{\rm top} = R_\odot$ define the boundaries of region where the flow is confined. The coupling matrix in Eq. (3) calculated for the flow defined above is proportional to u_0. Hence using Eq. (4), we have the frequency shift, $\delta\nu \propto u_0^2$.

3. Results

As explained in CA09, this calculation is little more involved as a non-zero t allows coupling between different m and m' of the p-modes. According to the selection rules imposed by the Wigner 3j symbols, the $s = 16, t = 16$ flow couples the mode (n, l, m) with $(n', l', m\pm16)$. Hence it becomes important to take into account the effect of rotational splitting on Δ before calculating the effect of these kind of poloidal flows. Thus, the difference of the square of frequencies, Δ is no longer independent of m. The couplings within a multiplet i.e., $(n, l, m) \rightleftarrows (n, l, m \pm 16)$ happen to be zero because of the anti-symmetry of the matrix elements (see Eqs. (16)-(18) in CA09).

In the upper panel of Fig. 1, we show the frequency shift of the mode with $(n, l) = (11, 38)$ due to coupling with $(10, 46)$. From Eq. (4), we have the frequency shift, $\delta\nu \propto 1/\Delta$. The $\delta\nu(m)$ shows a discontinuity at $m = 0$ since Δ for the $(11, 38, m) \rightleftarrows (10, 46, m - 16)$ becomes zero at $m = 0$ as shown in the lower panel. The reader is encouraged to compare this figure with Fig. 7 of CA09 where they plot similar curves for coupling of the modes $(18, 61, m) \rightleftarrows (17, 69, m\pm8)$. It is these discontinuities which give rise to a large value of splitting coefficients, a_q. Also notice the asymmetry of $\delta\nu(m)$ about $m = 0$ in Fig. 1. This means that not only the even coefficients, a_{2q} but also the odd coefficients, a_{2q+1} are non-zero. Usual inversion procedure for rotation neglects giant cells and assumes that the odd splitting coefficients arise only from rotation. If there are additional contributions to these coefficients, rotation inversions may not give correct results. In CA09, we performed a 1.5d rotation inversion on odd coefficients a_1 and a_3 to detect any discernible feature in the inverted profile. However, since the magnitude of the features in the inverted profile are smaller than the inversion errors we concluded that giant cells with $u_0 \leq 100$ m s^{-1} do not have much effect on the rotation inversion. The splitting coefficients a_1, a_2 and a_3 as a function of lower turning point radius and normalised by corresponding errors in the observational data from GONG are shown in Fig. 2. One can easily compare these coefficients for $s = 8, t = 8$ and $s = 16, t = 16$ flows. While the $Y_8^8(\theta, \phi)$ flow with an amplitude of $u_0 = 100$ m s^{-1} already produces a maximum a_2 which is twice the observational error, a Y_{16}^{16} flow with an amplitude $u_0 = 300$ m s^{-1} produces a maximum a_2 which is half the observational error. A similar thing may be said about the coefficients a_1 and a_3 as well. However, we have not performed a 1.5 D inversion for the $s = 16, t = 16$ case. We do not see a clear signal of 'nearly degenerate' modes in the observational data. Hence, like in CA09, in order put an upper limit on the amplitude of the flows we compare the a_2 values from theory with observational errors to calculate the confidence level of the upper limit. For the $Y_{16}^{16}(\theta, \phi)$, the confidence limit estimated by maximum value of a_2/σ_2 is less than 0.6 for a flow with an amplitude $u_0 = 300$m s^{-1} for several GONG data sets. In terms of the maximum radial velocity, $u_r^{\rm max} \sim 180$m s^{-1}. Thus banana cells with such amplitudes cannot be ruled out using the GONG data sets used. Another interesting observation from Fig. 2 is the large values of a_q at $r_t \sim 0.7R_\odot$ for both $t = 8$ and 16. We have checked that this is not due to $r_b = 0.7R_\odot$, but is an intrinsic property of the solar model used. The rotation profile used to calculate the rotational splittings for $t \neq 0$ giant cell flows may also be responsible. Nevertheless, since we also see this behaviour for $s = 8, t = 0$ flow (see Fig. 5 of CA09), we may conclude that the modes which have their turning points near the base of the convection zone are coupled strongly due to such poloidal flows.

4. Conclusions

We have calculated the effects of giant cells with an azimuthal degree 16 on p-mode splitting coefficients. We use the technique outlined in Chatterjee & Antia (2009) to perform this
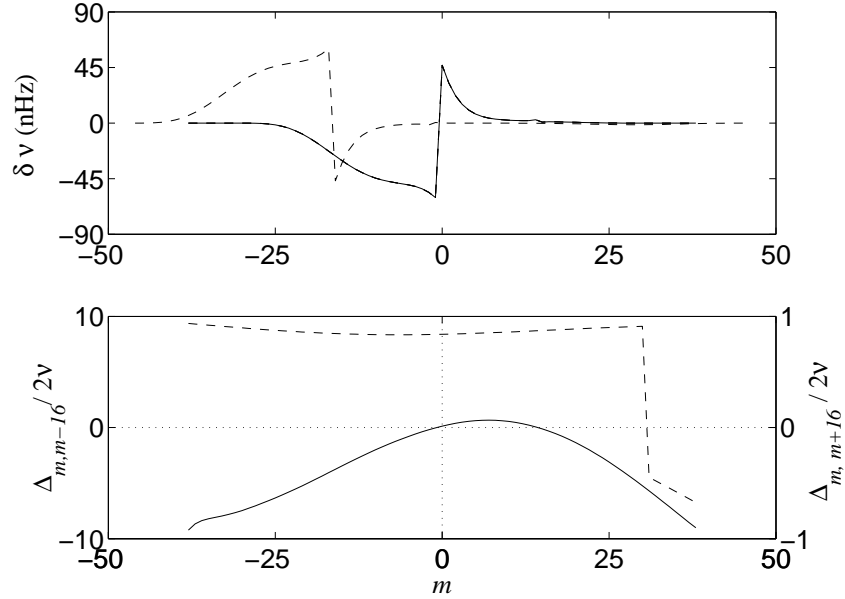
Figure 1. Upper panel: The *solid line* gives the frequency shift because of interaction between modes $(11, 38, m)$ having lower turning radius $r_t = 0.69 R_\odot$ and $(10, 46, m \pm 16)$ having $r_t = 0.74 R_\odot$, due to the flow with an angular dependence $Y_{16}^{16}(\theta, \phi)$. The frequency shift for the mode $(10, 46)$ is given by the *dashed line*. Lower panel: $\Delta_{m,m-16}/2\nu$ (*solid line*) for the coupling $(11, 38, m) \rightleftarrows (10, 46, m - 16)$; and $\Delta_{m,m+16}/2\nu$ (*dashed line*) for the coupling $(11, 38, m) \rightleftarrows (10, 46, m + 16)$. These values are in μHz.

calculation. We find that from observations we cannot rule out the existence of giant cells with an angular variation $Y_{16}^{16}(\theta, \phi)$ and an amplitude of $u_0 = 300$ m s^{-1} since the splitting coefficients are less than the observational errors. It is important to remember that $a_q \propto u_0^2$. In other words we can say that a flow varying as $Y_8^8(\theta, \phi)$ in the Sun can be ruled out with a confidence level estimated by the maximum value of the ratio $a_2/\sigma_2 \sim 2$ which is 30 times more than the confidence level for a flow varying as $Y_{16}^{16}(\theta, \phi)$ with the same amplitude $u_0 = 100$ m s^{-1}. Speaking in terms of maximum vertical velocity, u_r, according to Eq. (6), a $u_0 = 100$ m s^{-1} for a $s = 8, t = 8$ flow corresponds to $u_r^{\max} = 50$ m s^{-1} whereas for a $s = 16, t = 16$ flow implies a $u_r^{\max} = 60$ m s^{-1}.

We do not find any evidence from global helioseismology which may point at the appearance of banana cells with an azimuthal degree $t = 16$ in the DNS to being just an artifact of insufficient grid resolution. But we believe that in the DNS the velocity spectra would peak at the wavenumbers of the banana cells since they are so visually conspicuous in contrast to observations where there is no clear peak at giant cell scales. This may be because we do not resolve very many scales smaller than the banana cells in the DNS. But it is important to remember that we have used very regular analytical expressions for the banana cells. In the Sun, the cells will not only be irregular but also have finite lifetimes. The GONG data sets are averaged over 108 days and this may be somewhat longer than the lifetimes of giant cells and hence the signal may be averaged out. We can look at shorter data sets, but in that case the errors would be larger.

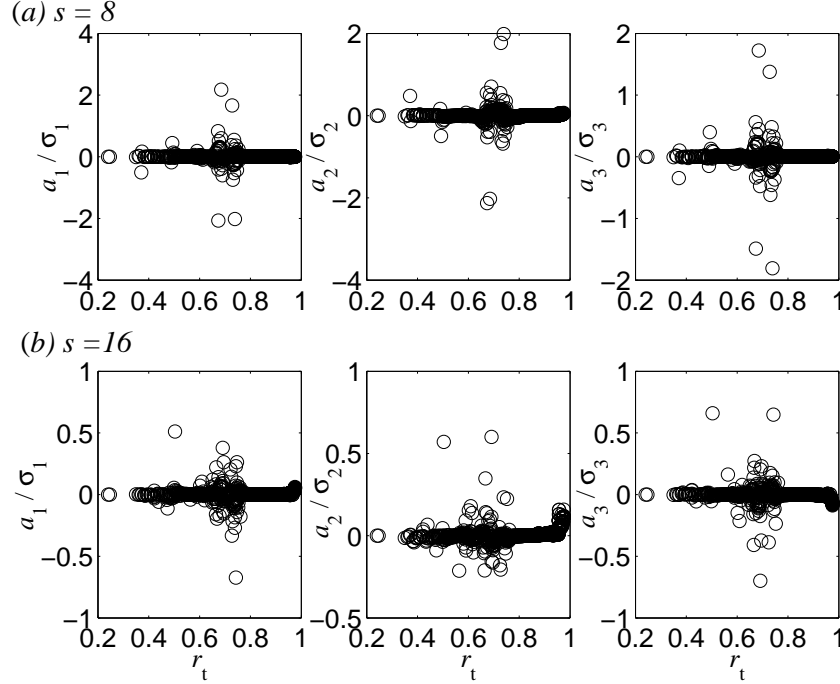(a) s = 8

(b) s = 16

Figure 2. (a) a_1/σ_1, a_2/σ_2 and a_3/σ_2 as a function of lower turning point radius r_t for the $Y_8^8(\theta, \phi)$ kind of flow with $u_0 = 100$ m s^{-1}. (b) Same as above but for a flow varying as $Y_{16}^{16}(\theta, \phi)$ with $u_0 = 300$ m s^{-1}. The σ_1, σ_2 and σ_3 are the errors in the corresponding observational splitting coefficients a_1, a_2 and a_3 from the GONG data set centered about November 2002.

[1] Beck, J.G., Duvall, T.L. Jr. and Scherrer, P.H. 1998 *Nature* **394** 653
[2] Canuto, V.M. and Mazzitelli, I. 1991 ApJ **370** 295
[3] Chatterjee, P. and Antia, H.M. 2009 ApJ **707** 208
[4] Chiang, W.-H. , Petro, L.D. and Foukal, P.V. 1987 *Solar Phys.* **110** 129
[5] Chou, D.-Y., LaBonte, B.J., Braun, D. C. and Duvall, T.L., Jr. 1991 ApJ **372** 314
[6] Edmonds, A.R. 1960 *Angular momentum in quantum mechanics* (Princeton University Press)
[7] Hathaway, D.H., Gilman, P.A., Harvey, J.W., Hill, F., Howard, R.F., Jones, H.P., Kasher, J.C., Leibacher, J. W., Pintar, J.A. and Simon, G.W. 1996 *Science* **272** 1306
[8] Hathaway, D.H., Beck, J.G., Bogart, R.S., Bachmann, K.T., Khatri, G., Petitto, J.M., Han, S. and Raymond, J. 2000 *Solar Phys.* **193** 299
[9] Iglesias, C.A. and Rogers, F.J. 1996 ApJ **464** 943
[10] Käpylä, P.J., Korpi, M., Guerrero, G., Brandenburg, A. and Chatterjee, P. 2010 *Preprint* (arXiv:1010.1250)
[11] LaBonte, B.J., Howard, R.F. and Gilman, P.A. 1981 ApJ **250** 796
[12] Lavely, E.M. and Ritzwoller, M.H. 1992, *Phil. Trans. Roy. Soc. Lon. A.* **339** 431
[13] Miesch, M.S., Brun, A.S. and Toomre, J. 2006 ApJ **641** 618
[14] Miesch, M.S., Brun, A.S., DeRosa, M.L. and Toomre, J. 2008 ApJ **673** 557
[15] Ritzwoller, M.H. and Lavely, E. M. 1991 ApJ **369** 557
[16] Rogers, F.J. and Nayfonov, A. 2002 ApJ **576** 1064
[17] Roth, M., Howe, R. and Komm, R. 2002 A & A **396** 243
[18] Simon, G.W. and Strous, L.H. 1997 *Bull. Am. Astron. Soc.* **29** 1402
[19] Snodgrass, H.B. and Howard, R. 1984 ApJ **284** 848

[20] Straus, T. and Bonaccini, D. 1997 A& A **324** 704

[21] Wang, H. 1989 *Solar Phys.* **123** 21